Application of ZnO Nanorods Based Whispering Gallery Mode Resonator in Optical Immunosensors

Alla Tereshchenko[b]*, G. Reza Yazdi[c], Igor Konup[d], Valentyn Smyntyna[a], Volodymyr Khranovskyy[c], Rositsa Yakimova[c], Arunas Ramanavicius[b]*

[a] *Department of Experimental Physics, Faculty of Mathematics, Physics and Information Technologies, Odesa National I.I. Mechnikov University, Pastera 42, 65023, Odesa, Ukraine;*
[b] *Department of Physical Chemistry, Institute of Chemistry, Faculty of Chemistry and Geosciences, Vilnius University, Naugarduko 24, LT-03225 Vilnius, Lithuania;*
[c] *Department of Physics, Chemistry and Biology, Linköping University, 58183 Linköping, Sweden;*
[d] *Department of Microbiology, Virology and Biotechnology, Faculty of Biology, Odessa National I.I. Mechnikov University, 2, Shampanskiy Lane, 65000, Odesa, Ukraine*

* Corresponding authors: Dr. Alla Tereshchenko, e-mail: alla_teresc@onu.edu.ua; and
Prof. habil. dr. Arunas Ramanavicius, e-mail: Arunas.Ramanavicius@chf.vu.lt

Abstract

In this research a whispering gallery mode (WGM) resonator based on vertically oriented ZnO nanorods, which were formed on silicon surface (siilcon/ZnO-NRs), has been applied in the design of optical immunosensor that was dedicated for the determination of grapevine virus A-type (GVA) proteins. Vertically oriented ZnO-NRs were grown on silicon substrates by atmospheric pressure metal organic chemical vapor deposition (APMOCVD) and the silicon/ZnO-NRs structures formed were characterized by structural and optical methods. Optical characterization demonstrates that silicon/ZnO-NRs-based structures can act as Whispering Gallery Mode (WGM) resonator where quasi-whispering gallery modes (quasi-WGMs) are generated. These quasi-WGMs were experimentally observed in the visible and infrared ranges of the photoluminescence spectra. In order to design an immune-sensing system the anti-GVA antibodies were immobilized on the surface of silicon/ZnO-NRs and in this way silicon/ZnO-NRs/anti-GVA structure was formed. The immobilization of anti-GVA antibodies and then the interaction of silicon/ZnO-NRs/anti-GVA structure with GVA proteins (GVA-antigens) resulted in an opposite shifts of the WGMs peaks in the visible range of the photoluminescence spectra observed as a defect-related photoluminescence emission of ZnO-NRs. Here designed silicon/ZnO-NRs/anti-GVA immune-sensing structure demonstrates the sensitivity towards GVA-antigens in the concentration range of 1-200 ng/ml. Bioanalytical applicability of the silicon/ZnO-NRs-based structures in the WGMs registration mode is discussed.

1. Introduction

Among the variety of ZnO-based nanostructures that have been demonstrated, the one-dimensional ZnO-nanorods (NRs) with hexagonal wurtzite structure and high crystalline quality have become one of the most frequently used nanostructure, which is also well suited for biosensors design [1,2]. The fundamental properties of ZnO as a semiconductor, such as the direct wide band gap (E_g ~3.37eV) and strong photoluminescence, complemented by a high surface-to-volume-ratio of its nanostructures along with its biocompatibility, make ZnO-NRs largely desired in a variety of biosensors: electrical, electrochemical, optical and some others [1,2,3]. Due to the large excitonic binding energy (~60 meV) and an intense photoluminescence at room temperature, ZnO-NRs are widely used in optical biosensors. Optical transduction is an attractive technique for biosensing due to its high sensitivity and specificity, applicability in real-time monitoring, capability for high throughput and simple sample pre-treatment. Therefore, optical transduction is a good alternative to electrochemical and piezoelectric determination of the analytical signal [4]. Both label-free and labelled determinations of the target analyte are possible by ZnO-based optical transducers [1]. Among many other optical approaches, photoluminescence is one of the most sensitive and simple method [1,5,6]. The photoluminescence-based sensors mostly are based on photoluminescent material, which is acting as a transducer due to its ability to convert molecular interactions into the variation of a photoluminescence-signal [7]. ZnO-NRs are forming hexagonal 'optical resonator' inside which light can circulate in cyclic manner due to a total internal reflection at the boundaries between ZnO-NRs and air, therefore, ZnO-NRs can act as a resonator of whispering gallery modes (WGMs) [8]. Various ZnO micro- and nanostructures with such hexagonal cross-sections are mostly applied in photonic devices as optical resonators, which are useful for laser-based optoelectronics [9,10,11,12] and biosensorics [13,14]. Also, some studies utilizing WGMs for biosensorics are based on microspheric optical resonators, formed by ZnO-based structures [12,13,15,16]. The registration of WGMs enables highly sensitive label-free detection of changes in surrounding refractive index [12] or generation of photoluminescence signal [13]. Therefore, recent theoretical insights in the formation of WGMs encourage the development of label-free WGMs-based analytical systems suitable for the determination of some analytes [17,18].

This paper is focused on optical characterization of vertically oriented ZnO-NRs grown on silicon by atmosphere pressure metal organic chemical vapor deposition method. The optical characterization demonstrates that the obtained silicon/ZnO-NRs can act as a WGM resonator where the WGMs are experimentally observed in the visible and near infrared ranges of the photoluminescence spectra. An immune-sensing platform based on silicon/ZnO-NRs structures, which were acting in WGMs generation mode, has been designed. This platform was dedicated to the determination of grapevine virus A-type (GVA) proteins (GVA-antigens).

2. Materials and Methods

2.1. Formation and characterization of ZnO-NRs/silicon structures

ZnO nanostructured layers were grown on silicon substrates by APMOCVD at 500 $^{\circ}$C. As can be seen from the cross-sectional SEM image (Fig. 1a), during growth first a continuous ZnO-layer was formed on the silicon substrate and then vertically oriented ZnO-NRs were grown on initially formed ZnO-layer (Fig. 1).

To study the surface morphology, structural and optical properties of the samples we applied different characterization techniques: scanning electron microscopy (SEM), atomic force microscopy (AFM), X-ray diffraction (XRD) and photoluminescence spectroscopy. The microstructure of the silicon/ZnO-NRs was studied by (SEM) using a Leo/Zeiss 1550 Gemini SEM from Carl Zeiss AG (Oberkochen, Germany) operated at voltages ranging from 10 to 20 kV and using a standard aperture value of 30 μm.

Chemical composition of the samples was determined by ZEISS EVO 50 XVP using energy dispersive X-ray spectroscopy (EDX) furnished INCA 450 from OXFORD Instruments (Oxford, UK). The operating voltage for EDX analysis was set to 20 kV. AFM was performed using a Dimension 3100 from Digital Instruments/Veeco (Santa Barbara, USA) operated in tapping mode.

The crystal phase analysis of the ZnO-NRs/silicon samples was performed by XRD *via* acquiring θ-2θ scans using a Philips PW 1825/25 diffractometer, utilizing Cu-Kα radiation (λ = 0.1542 nm). The XRD spectra displayed only one single peak at 34.44° related to (001) plane reflection, confirming the single phase ZnO of wurtzite structure.

Optical properties of silicon/ZnO-NRs were characterized by photoluminescence measurements using solid state laser with excitation wavelength of 355 nm and excitation power of 1.2 mW. ZnO photoluminescence from an area of 0.4 by 0.4 mm entered a spectrometer with the slit entrance of 1 by 1 mm, a focal length of 550 and a liquid nitrogen cooled CCD as the detector. An excitation area of 0.4 mm wide was evaluated in order to obtain an average photoluminescence signal of each sample. The diameter of the laser spot on the sample surface was around 1 mm and the angle of incidence was about 20°. All photoluminescence experiments were recorded at room temperature, with a spectral resolution of 3.3 nm, using the spectrometer

TRIAX 550 from HORIBA/Jobin Yvon (Bensheim, Germany). [7]. The laser was blocked by a 364 nm long pass filter after the sample, with full transmission from 368 nm.

2.2. Functionalization of silicon/ZnO-NRs structures by proteins

The biological samples used for protein modification of ZnO-NRs were kindly provided by the National Scientific Centre 'Institute of Viticulture and Wine Making named after V. Ye. Tairov' (Odesa, Ukraine). The used proteins were part of the immunoassay-based KIT for the determination of Grapevine virus A-type (GVA) produced by 'Agritest' (Valenzano, Italy) and consisted of anti-GVA antibodies (anti-GVA) containing serum, which indeed was a real sample extracted from GVA-infected grape plants and a control sample of GVA antigens, containing extract of GVA-infected grape plants (GVA-antigens).

The anti-GVA antibody immobilization procedure was the following: 5 μl of anti-GVA antibodies containing sample was diluted 200 times (it corresponds to 1/200 dilution of initial sample) by dissolving in 0,01 mol/l PBS, pH 7.4. Then this solution was equally distributed on the surface of the silicon/ZnO-NRs samples and was incubated for 1h in humid environment at room temperature. After this, modified silicon/ZnO-NRs samples were washed with PBS and with deionized water and then they were dried in air for 1h at room temperature and in such a way a silicon/ZnO-NRs/anti-GVA-based structure was formed. Then the photoluminescence signal of the silicon/ZnO-NRs/anti-GVA structure was registered. In order to determine the interaction of the silicon/ZnO-NRs/anti-GVA structure with GVA-antigens the silicon/ZnO-NRs/anti-GVA slide was incubated in GVA-antigen containing solution for 30 min followed by washing in deionized water, dried and then similar as above photoluminescence procedure was applied for determination of the silicon/ZnO/anti-GVA/GVA-antigen photoluminescence signal.

3. Results and Discussion

The SEM image (Fig. 1a) illustrates that silicon/ZnO-NRs were vertically oriented to the silicon substrate, having the average dimensions of 200 nm in diameter and up to few micrometers in length. The EDX analysis has shown the equal presence of zinc and oxygen in the formed samples and only very small amount of Mn, which was used in the CVD process as a dopant that was added in all the samples. Figure 1b represents the cross-section image of the silicon/ZnO-NRs, along with the data obtained by EDX mapping – thus every dot corresponds to a specific element (Zn, O, Mn etc) marked by specific color that demonstrates also the microstructure of the nanorods and their uniformity in terms of elements. Mn doping was performed in order to get vertically oriented ZnO nanorods with intense visible photoluminescence. It was observed experimentally that the addition of some forensic dopants during the APMOCVD-based procedure changes the film formation kinetics and alters the growth regime to vertical nanorods. Besides, the intrinsic ZnO, when it has high crystal quality, usually demonstrates high UV

emission due to near band edge (NBE) transitions and weak visible luminescence, therefore Mn was used as a dopant of ZnO. Mn creates deep level defects, which affect the luminescence spectrum of the material and provide visible emission within 450 - 650 nm, as well as emission within 590 - 630 nm, which is determined by the nature of the dopant and in our case it overlaps with the defect-related photoluminescence emission of ZnO.

AFM investigation of the silicon/ZnO-NRs morphology has confirmed SEM-based observations. The average of root mean square (Rms) roughness calculated from AFM images is 35 nm (Fig. 1c).
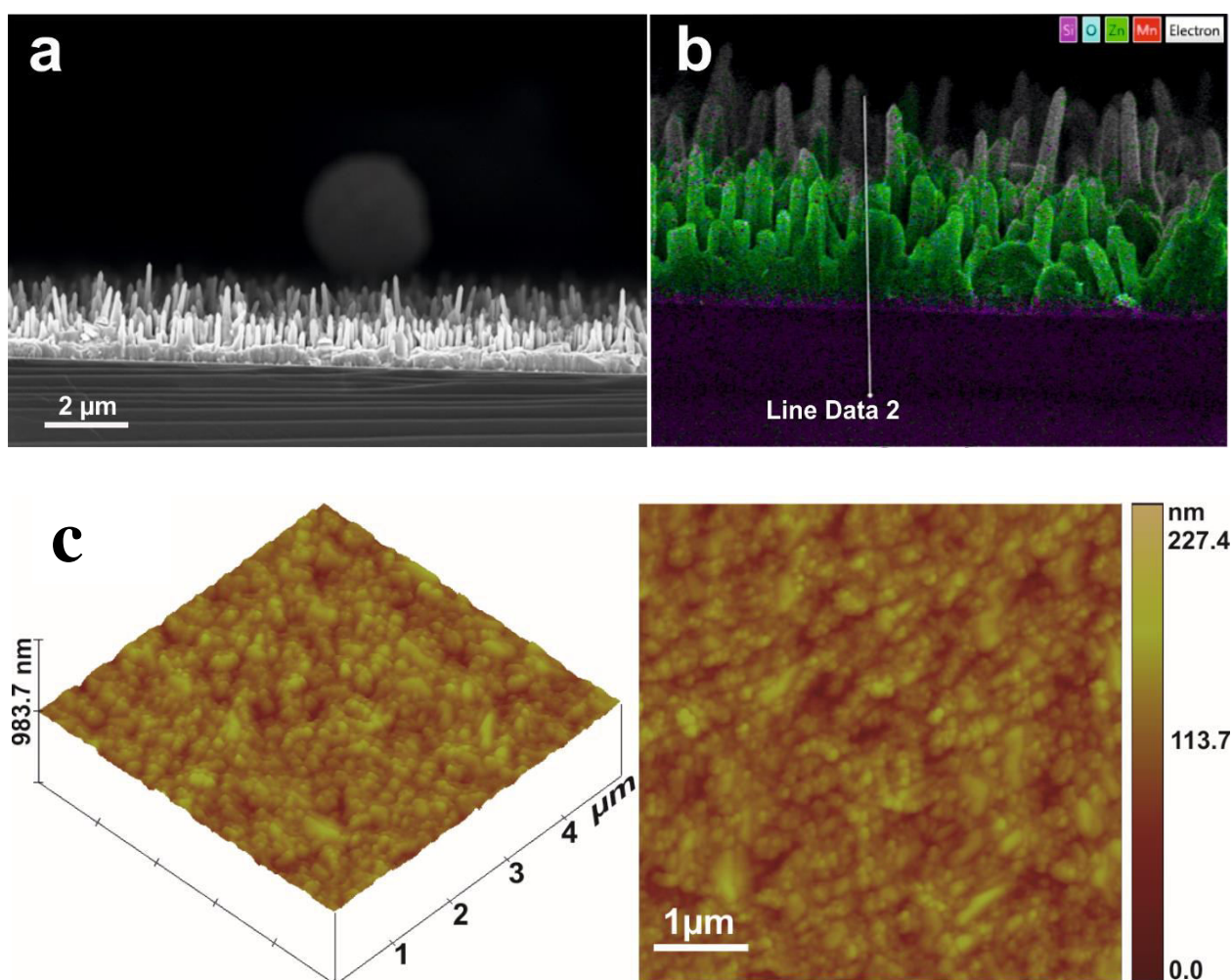

Figure 1. a) SEM image of silicon/ZnO-NRs; b) EDX spectroscopy based elemental analysis of silicon/ZnO-NRs; c) AFM images of silicon/ZnO-NRs.

The photoluminescence spectra of silicon/ZnO-NRs were characterized by an intense near band edge (NBE) peak centered at 378 nm and by an extraordinary form of the photoluminescence emission in the visible range that was observed as defect-related photoluminescence of silicon/ZnO-NRs (Fig. 2a). As we suggest, optical resonance standing waves, known also as Whispering Gallery Modes (WGMs), were generated inside the layer formed out of silicon/ZnO-NRs that created a regularly shaped optical resonator where WGMs can be excited [8,9]. This effect is induced by the morphology of the samples i.e. vertically grown silicon/ZnO-NRs with rather uniform shape and orientation. The hexagonal structure of the vertically oriented silicon/ZnO-NRs, irradiated by UV light (355 nm) with particular incidence angle, creates in some silicon/ZnO-NRs based optical resonator the WGMs when the light is reflected from each facet and inside of the WGM resonator it is propagating in 'spiral-way', which is determined by the incidence angle of ~20° *vs* the plane of the substrate on which silicon/ZnO-NRs are formed. Such conditions of the photoluminescence measurements enable to observe the so called 'quasi-WGMs' [19], when WGMs are generated by light-path inside of the hexagonal WGM resonator formed in silicon/ZnO-NRs. An envelope curve of the WGM peaks in the visible range forms a defect-related (deep level) photoluminescence emission of silicon/ZnO-NRs deposited by APMOCVD, centered at around 525 nm, similarly to the results described in other studies [20]. The Gaussian fitting of the envelope curve of the WGM peaks in the visible range indicates the maximum of photoluminescence emission at 528 nm (Fig. 2b), the standard error, which is indicated in the inset, is about 2.5 nm. The schematic illustration of WGMs light path generated inside the silicon/ZnO-NRs is shown in Figure 3. In the most of the crystal structures quasi-WGMs are hardly observable due to the low quality factor (Q) and therefore they are not frequently investigated. Therefore, here presented results, which demonstrate that even the ZnO-NRs of such small diameter (200 nm) can serve as a WGM resonator where quasi-WGMs can be excited, have a significant scientific value. By this research we are demonstrating that silicon/ZnO-NRs is an additional type of WGM resonator that can be used for WGMs excitation. It should be noted that Figure 3 represents a simplified illustration of the WGMs light path in hexagonal ZnO-NRs based resonator. In our case, we excite samples containing multiple non strictly parallel ZnO-NRs among which some will meet the optical rules of internal reflection appropriate for the formation of WGMs.

The intensity of the NBE peak of the samples was found to vary from 20000 to 40000 a.u. that caused by an increase of silicon/ZnO-NRs layer thickness along the silicon substrate. The intensity and amplitude of standing waves, which are reflected in WGMs, were also a little bit different within all silicon/ZnO-NRs samples, as well as the position, intensity and number of WGMs peaks that are presented in Figures 2 and 4. The latter can be caused by the distribution of diameter of ZnO-NRs formed on the silicon substrate and due to the fact that the morphology and size of an WGM resonator greatly affect the energy and resonance levels of the resonant modes [21].
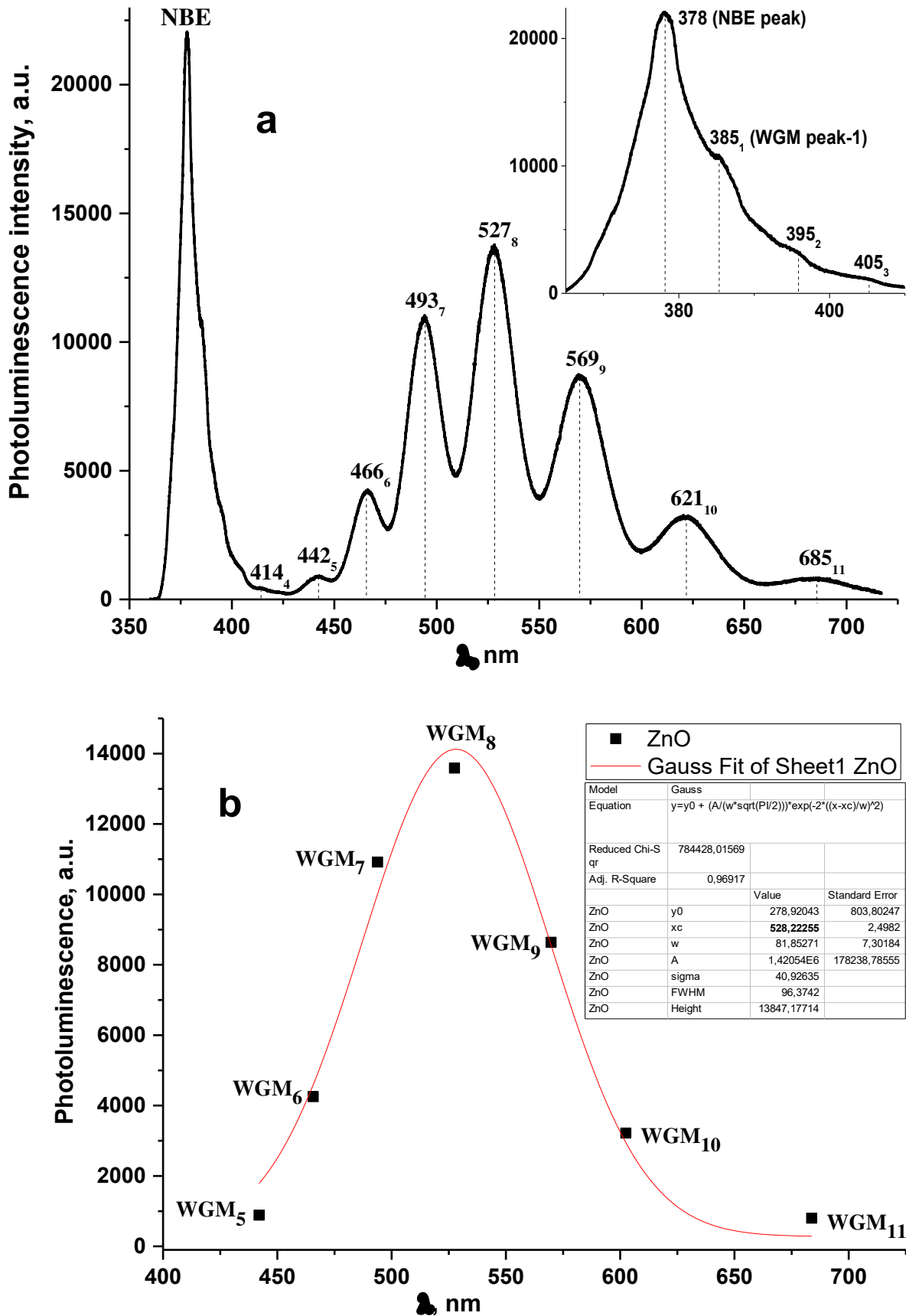
Figure 2. Photoluminescence spectra of silicon/ZnO-NRs with WGMs generated inside of optical resonators formed in the silicon/ZnO-NRs structure (a); Gaussian fitting of an envelope curve of the WGMs peaks in the visible range of the photoluminescence spectra (b).
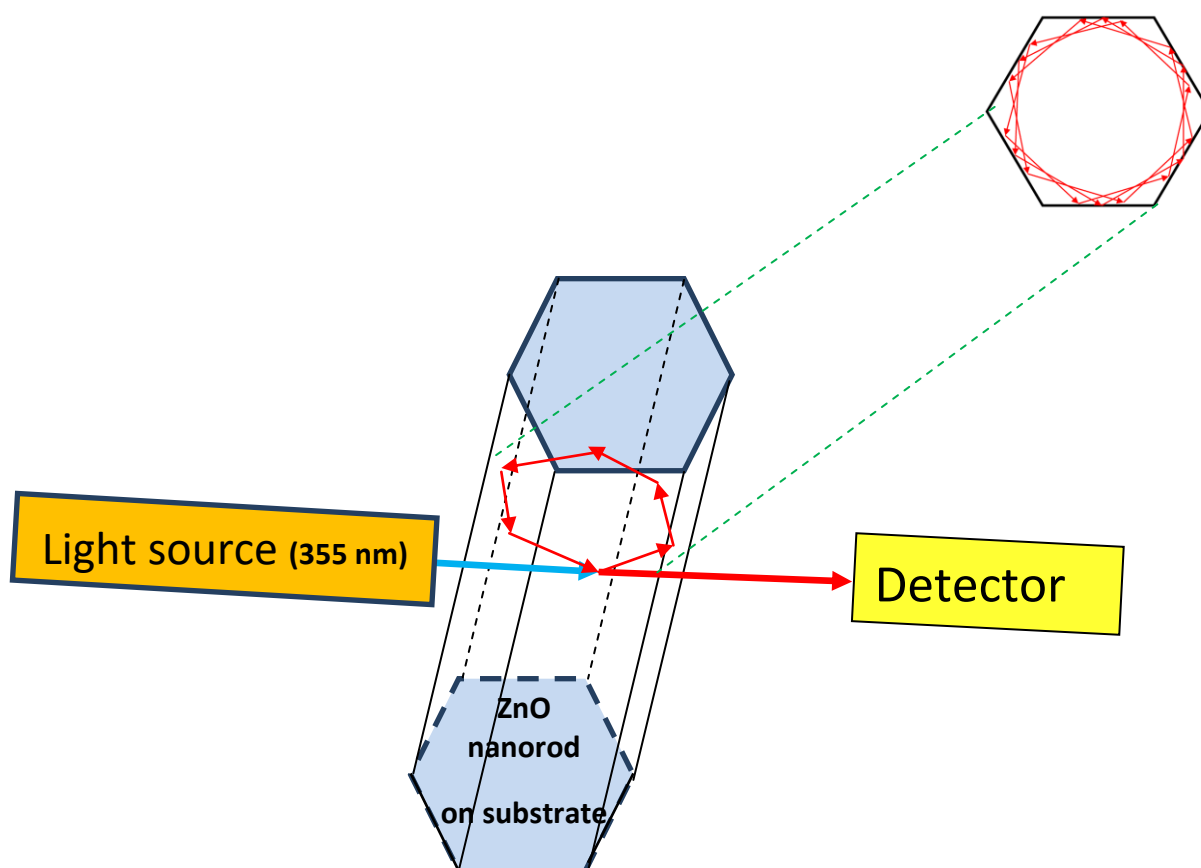
Figure 3. Simplified schematic illustration of the WGMs optical-paths generated inside ZnO-NRs.

3.1. Generation of WGMs in silicon/ZnO-NRs modified by proteins

In order to investigate the possibility to apply silicon/ZnO-NRs, which are generating WGMs, in the design of immunosensors, the surface of the silicon/ZnO-NRs structures were modified by anti-GVA antibodies, which are selectively recognizing GVA-antigens. The immobilization procedure of the anti-GVA antibodies on the surface of the silicon/ZnO-NRs was similar to the one described by the authors in the previous research [7]. However, the incubation of as-grown silicon/ZnO-NRs in several solutions containing different anti-GVA antibody concentrations (solutions prepared by 1/200, 1/100 and 1/50 dilution of initial anti-GVA antibody containing sample) did not result in substantial changes of the photoluminescence spectra. The surface of

as-grown silicon/ZnO-NRs structures was determined to be very hydrophobic and no changes in the photoluminescence signal after anti-GVA immobilization were observed what enabled an effective immobilization of proteins by simple adsorption on silicon/ZnO-NRs structures. However, such strong adsorption of proteins increased the probability of nonspecific interactions, therefore, this kind of hydrophobic silicon/ZnO-NRs structures was not suitable for the design of an immune-sensing platform. Therefore, in order to make the surface of ZnO-NRs less hydrophobic, the samples were irradiated by UV illumination with excitation source of 255 nm during 30 min [22,23].

The immobilization of anti-GVA antibodies on the surface of the UV-irradiated silicon/ZnO-NRs of the initial anti-GVA sample diluted by 1/200 ratio resulted in several effects: (i) an increase of the NBE peak intensity of silicon/ZnO-NRs by 15.5 % in average, which has been typically observed in many researches [7,24]); (ii) the appearance of a new photoluminescence band in the region from 400 to 450 nm, which is in line with the results reported in an earlier research [7]; and (iii) in the change of the position and intensity of WGMs peaks. Because after immobilization of anti-GVA antibodies and after interaction of silicon/ZnO-NRs/anti-GVA-based immune-sensing platform with GVA antigens the positions of each WGM peak changed non-equally, the 'Gauss fitting curves' were plotted for each photoluminescence spectrum and are shown on the insets of Figures 4a, 4b and 4c in order to analyze the defect-related photoluminescence emission band of the ZnO-NRs (Fig. 1, 2 and 3 in Supplementary Materials). Immobilization of anti-GVA antibodies on the surface of ZnO-NRs resulted in the UV-shift of defect-related photoluminescence emission of 4 nm (Fig. 4a, inset), 10 nm (Fig. 4b, inset) and 22 nm (Fig. 4c, inset) observed for different ZnO-NRs samples. The full information on the plotted 'Gauss fitting curves', including standard error values, is presented in Figures S1b, S2b and S3b, respectively. The silicon/ZnO-NRs samples have demonstrated high reproducibility of the changes in photoluminescence signal, in particular, WGMs peaks positions and their intensity that have resulted after immobilization of anti-GVA antibodies on the surface of ZnO-NRs (9 repetitions, 7 % error).

Incubation of the silicon/ZnO-NRs/anti-GVA based immune-sensing platform in different concentrations of GVA-antigens, which are the target analyte in this research and specifically binds to immobilized for anti-GVA antibodies, resulted in some decrease of the NBE peak by 6% in average, which is typical for ZnO according to the other researches [7,19,25], and some IR shift of the WGMs peaks (Fig. 4a, b, c). When the silicon/ZnO-NRs/anti-GVA based immunosensing platform was incubated in solution containing low concentration (1 ng/ml) of GVA-antigens the integral intensity and absolute amplitude of WGMs has decreased comparably to that of the silicon/ZnO-NRs/anti-GVA (Fig. 4a). When silicon/ZnO-NRs/anti-GVA-based immunosensing platform was incubated in solution containing higher concentrations of GVA-antigens, then the integral intensity of registered WGMs has increased (Fig. 4 b, c), while the absolute WGMs amplitude remained almost the same (Fig. 4 b, c). The Gauss fitting based

approximations (Fig. S1, S2 and S3) demonstrate opposite changes in the defect-related photoluminescence band as a result of an interaction of anti-GVA immobilized on silicon/ZnO-NRs (silicon/ZnO-NRs/anti-GVA structure) with GVA-antigens – backward shift of the 'Gauss fitting curves' towards IR region by 2.5 nm (Fig. 4 a, inset), 4.4 nm (Fig. 4 b, inset) and 4.4 nm (Fig. 4 c, inset) for silicon/ZnO-NRs/anti-GVA immunosensing platforms incubated in solutions containing 1, 100 and 200 ng/ml concentrations of GVA-antigens, correspondently. The full information on the plotted Gauss fittings, including standard error values, is shown in the figures S1c, S2c and S3c, respectively. The silicon/ZnO-NRs/anti-GVA structure demonstrated good reproducibility of the changes in photoluminescence signal induced by interaction with target analyte – GVA-antigens i.e. 3 repetitions for each of GVA-antigen concentrations resulted in 6% 5% and 8 % error for 1 ng/ml, 100 ng/ml and 200 ng/ml concentrations, respectively.
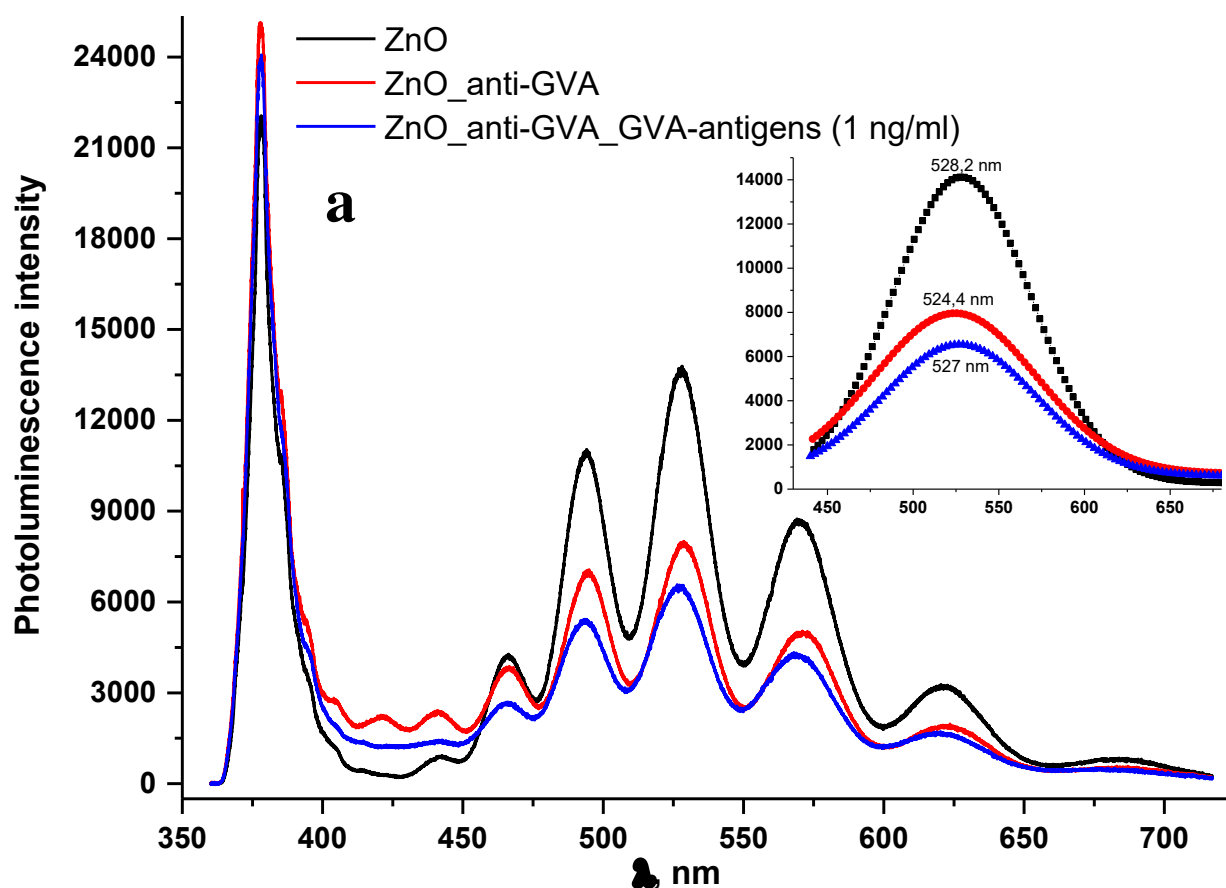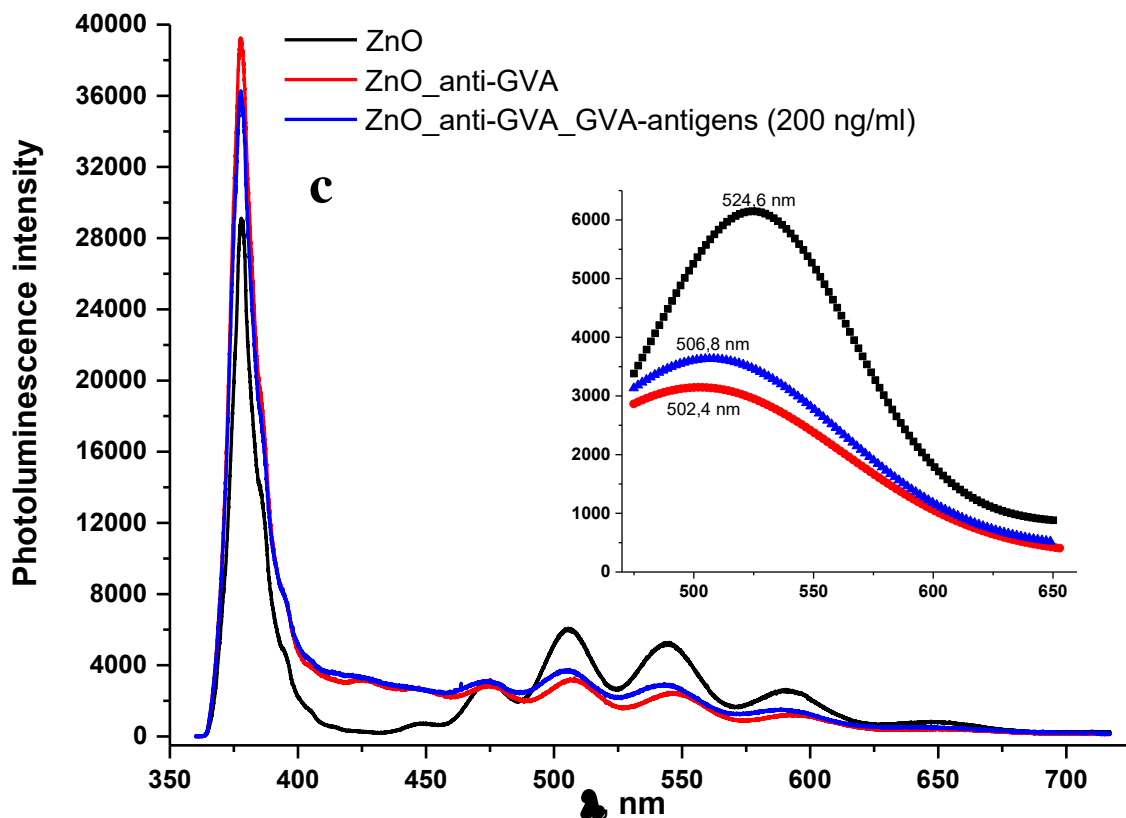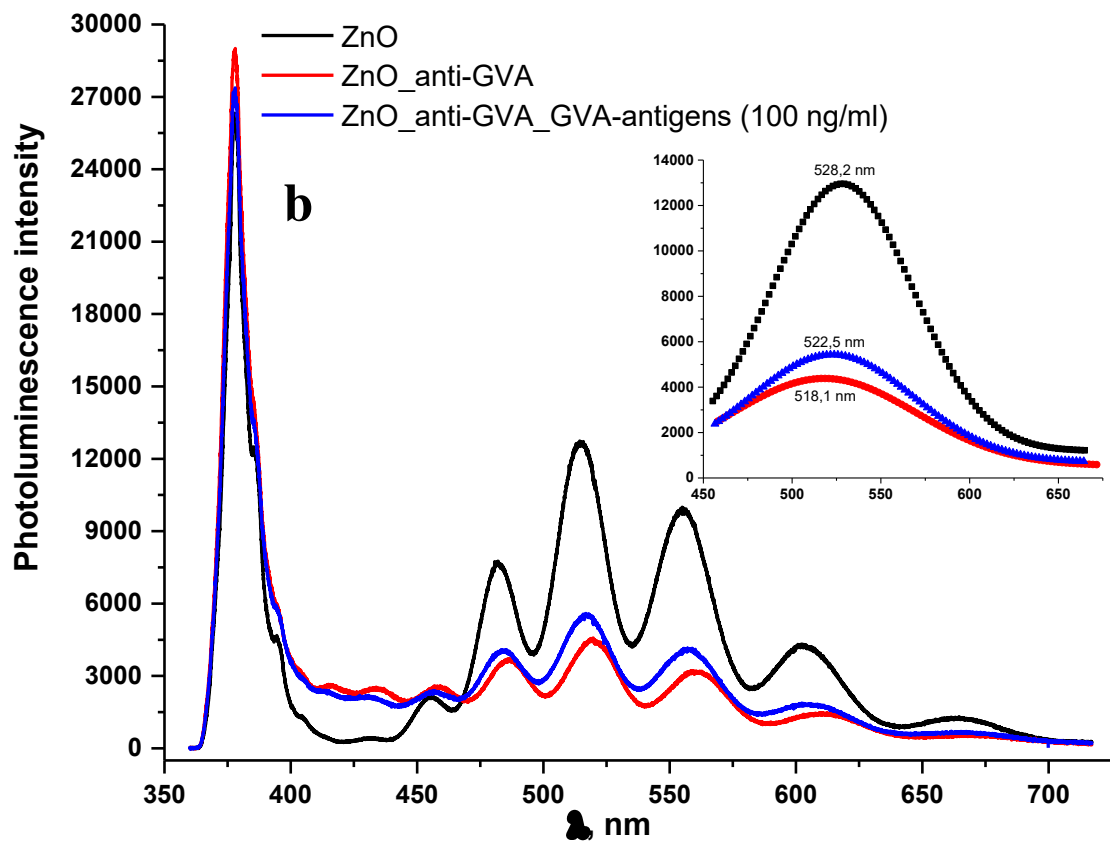
Figure 4. Photoluminescence spectra of silicon/ZnO-NRs and silicon/ZnO-NRs/anti-GVA based structures incubated in aliquots containing different GVA-antigen concentrations, namely: 1 ng/ml (a); 100 ng/ml (b); 200 ng/ml (c). The insets show the Gauss fittings of the envelope curves of WGMs peaks in the visible range of photoluminescence spectra.

Some aspects in the behavior of the photoluminescence emission in the visible range as a result of the modification of surfaces, which exhibits photoluminescence properties, by proteins was observed and discussed in some other studies [19,24,25]. The designed silicon/ZnO-NRs/anti-GVA immunosensing structure, which is generating WGMs, demonstrates sufficient sensitivity towards GVA-antigens down to 1 ng/ml. The redistribution of the initial photoluminescence signal generated by ZnO-NRs so far was not evaluated in detail, therefore, in this research we have not aimed to establish the exact calibration of silicon/ZnO-NRs/anti-GVA based immunosensing platform towards target analyte – GVA-antigens. Despite of this fact, the obtained results demonstrate a high potential for the application of ZnO-NRs in the design of immunosensors, where analytical signal is based on the assessment of the WGMs signal.

In order to prove experimentally the binding of GVA-antigens to the immobilized anti-GVA that are forming outer layer of a silicon/ZnO-NRs/anti-GVA structure, the AFM investigations of the silicon/ZnO-NRs modified by proteins was performed before the immobilization of immobilized anti-GVA layer and after the formation of anti-GVA/GVA-antigen complexes (Fig. 5). AFM images demonstrate different surface morphology based on filamentous flexuous particles [26,27] formed on the surface of the silicon/ZnO-NRs/anti-GVA/GVA-antigen structure (Fig. 5b), which we attribute to the formed anti-GVA/GVA-antigen complexes.
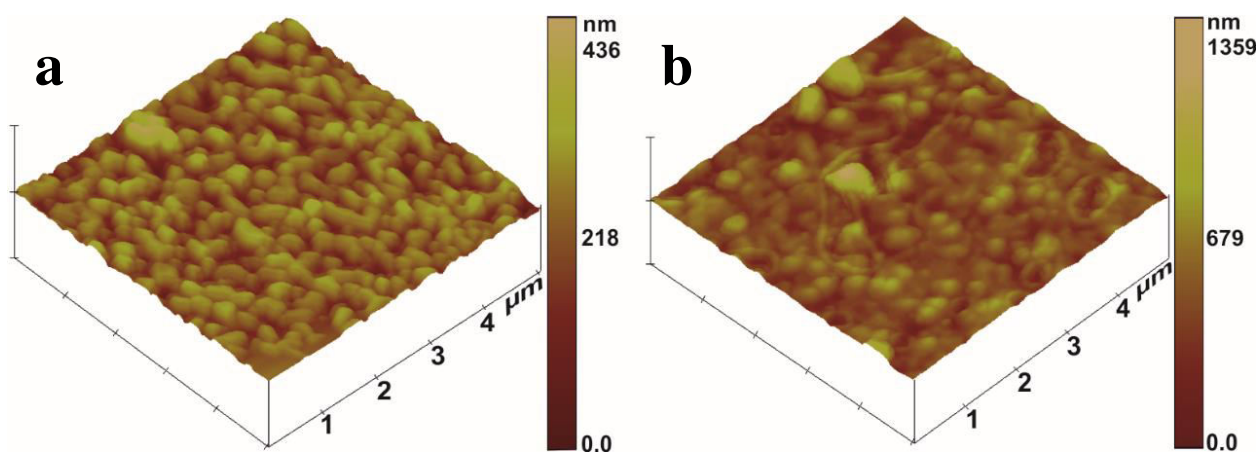
Figure 5. Silicon/ZnO-NRs (a); silicon/ZnO-NRs/anti-GVA immunosensing platform after the incubation in solution containing 100 ng/ml of GVA antigen (b).

4. Conclusions and future developments

The obtained results demonstrate that hexagonal ZnO-NRs of rather small diameter (200 nm), vertically oriented on the surface of silicon substrates, can serve as a WGMs resonator in which quasi-WGMs can be excited. The immobilization of anti-GVA antibodies on the surface of silicon/ZnO-NRs-based layer resulted in a UV shift of the WGMs peaks in the visible range of spectra. Further interaction of the biologically selective layer with GVA-antigens resulted in the opposite shift of the WGMs peaks observed as a defect-related photoluminescence emission of silicon/ZnO-NRs.

Registration of WGMs, excited within the optical resonator of ZnO-NRs enables the application of silicon/ZnO-NRs/anti-GVA immunosensing structure in the design of biosensors suitable for the determination of GVA proteins (GVA-antigens). The formed silicon/ZnO-NRs/anti-GVA immunosensor structure, which generates WGMs, shows a sensitivity towards GVA-antigens in a concentration range of 1-200 ng/ml. The obtained results demonstrate a high potential for the application of ZnO-NRs in the design of immunosensors, where the analytical signal is determined by the assessment of a WGMs-based signal. Therefore, we believe that future improvement of the silicon/ZnO-NRs formation procedure in order to obtain more uniform structures with well-defined optical parameters will allow the development of highly sensitive immunosensors based on the WGMs excited within optical resonators in ZnO-NRs-based layers.

Conflicts of Interest: The authors declare no conflicts of interests.

References

[1] A. Tereshchenko, M. Bechelany, R. Viter, V. Khranovskyy, V. Smyntyna, N. Starodub, R. Yakimova, Optical biosensors based on ZnO nanostructures: advantages and perspectives. A review, Sens. Actuators B 229 (2016) 664–677.

[2] R. Yakimova, L. Selegård, V. Khranovskyy, R. Pearce, A. Lloyd Spetz, K. Uvdal, ZnO materials and surface tailoring for biosensing, Front. Biosci. 4 (2012) 254–278.

[3] O. Graniel, M. Weber, S. Balme, P. Miele, M. Bechelany, Atomic layer deposition for biosensing applications, Biosens. Bioelectron 122 (2018) 147-159.

[4] J. Politi, I. Rea, P. Dardano, L. De Stefano, M. Gioffrè, Versatile synthesis of ZnO nanowires for quantitative optical sensing of molecular biorecognition, Sens. Actuators B 220 (2015) 705–711.

[5] S. N. Sarangi, S. Nozaki, S. N. Sahu, ZnO nanorod-based non-enzymatic optical glucose biosensor, J. Biomed. Nanotechnology 11 (2015) 988–996.

[6] S. Elhag, Z. H. Ibupoto, V. Khranovskyy, M. Willander, O. Nur, Habit-modifying additives and their morphological consequences on photoluminescence and glucose sensing properties of ZnO nanostructures, grown via aqueous chemical synthesis, Vacuum 116 (2015) 21-26.

[7] A. Tereshchenko, V. Fedorenko, V. Smyntyna, I. Konup, A. Konup, M. Eriksson, R. Yakimova, A. Ramanavicius, S. Balme, M. Bechelany, ZnO films formed by atomic layer deposition as an optical biosensor platform for the detection of grapevine virus A-type proteins, Biosens. Bioelectron 92 (2017) 763-769.

[8] J. Liu, S. Lee, Y. H. Ahn, J-Y. Park, K. H. Koh, K. H. Park, Identification of dispersion-dependent hexagonal cavity modes of an individual ZnO nanonail, Appl. Phys. Lett. 92 (2008) 263102.

[9] T. Nobis, M. Grundmann, Low-order optical whispering-gallery modes in hexagonal nanocavities, Phys. Rev. A 72 (2005) 063806.

[10] J. Dai, C. X. Xu, X. W. Sun, ZnO-microrod/p-GaN heterostructured whispering-gallery-mode microlaser diodes, Adv. Mater. 23 (2011) 4115–4119.

[11] C. Czekalla, T, Nobis, A. Rahm, B. Cao, J. Zuniga-Perez, Whispering gallery modes in zinc oxide micro- and nanowires, Phys. Status Solidi B 247 6 (2010) 1282–1293.

[12] C. Czekalla, C. Sturm, R. Schmidt-Grund, B. Cao, M. Lorenz, M. Grundmann, Whispering gallery mode lasing in zinc oxide microwires, Appl. Phys. Lett. 92 (2008) 241102.

[13] T. Reynolds, M. R. Henderson, A. François, N. Riesen, J. M. M. Hall, S. V. Afshar, S. J. Nicholls, T. M. Monro, Optimization of whispering gallery resonator design for biosensing applications, Opt. Express 23, 13 (2015) 17067-17076.

[14] R. S. Moirangthem, P.-J. Cheng, P. C.-H. Chien, B. Trong, H. Ngo, S.-W. Chang, C.-H. Tien, Y.-C. Chang, Optical cavity modes of a single crystalline zinc oxide microsphere, Opt. Express 21, 3 (2013) 3010-3020.

[15] N. Trong, P. Chien, Y.-D. Chen, S.-H. Wu, F.-C. Hsiao, L.-N. Nguyen, Y.-C. Chang, Whispering-gallery mode biosensor – a detailed study on ZnO microspheres, IFMBE Proceedings 46 (2015) 21-24.

[16] P. Listewnik, M. Hirsch, P. Struk, M. Weber, M. Bechelany, M. Jedrzejewska-Szczerska, Preparation and Characterization of Microsphere ZnO ALD Coating Dedicated for the Fiber-Optic Refractive Index Sensor, Nanomaterials 9, 2 (2019) 1-11.

[17] A. M. Armani, R. P. Kulkarni, S. E. Fraser, R. C. Flagan, K. J. Vahala, Label-Free, Single-molecule detection with optical microcavities, Science 317 (2007) 783-787.

[18] F. Wollmer, S. Arnold, Whispering-gallery mode biosensing: label-free detection down to single molecules, Nat. Methods 5, 7 (2008) 591–596.

[19] L. Sun, H. Dong, W. Xie, Zh. An, X. Shen, Z. Chen, Quasi-whispering gallery modes of excitonpolaritons in a ZnO microrod, Opt. Express 18, 15 (2010) 15371-15376.

[20] D. Sodzel, V. Khranovskyy, V. Beni, A.P.F. Turner, R. Viter, M.O. Eriksson, P.-O.Holtz, J.-M. Janot, M. Bechelany, S. Balme, V. Smyntyna, E. Kolesneva, L. Dubovskaya, I. Volotovski, A. Ubelis, R. Yakimova, Continuous sensing ofhydrogen peroxide and glucose via quenching of the UV and visible luminescence of ZnO nanoparticles, Michrochem. Acta 182 (2015) 1819 –1826.

[21] H. Dong, B. Zhou, J. Li, J. Zhan, L. Zhang, Ultraviolet lasing behavior in ZnO optical microcavities, J Materiomics 3 (2017) 255-266.

[22] S. Hoshian, V. Jokinen, K. Hjort, R. H. A. Ras, S. Franssila, Amplified and localized photoswitching of TiO2 by micro – and nanostructuring, ACS Appl. Mater. Interfaces 7, 28 (2015) 15593–15599.

[23] H. Chen, Y. Liu, C. Xie, J. Wu, D. Zeng, Y. Liao, A comparative study on UV light activated porous TiO2 and ZnO film sensors for gas sensing at room temperature, Ceram. Int. 38 (2012) 503–509.

[24] A. Tereshchenko, V. Smyntyna, A. Ramanavicius, Interaction mechanism between TiO2 nanostructures and bovine leukemia virus proteins in photoluminescence-based immunosensors, RSC Advances, 8, 2018, 37740–37748.

[25] R. Viter, M. Savchuk, N. Starodub, Z. Balevicius, S. Tumenas, A. Ramanaviciene, D. Jevdokimovs, D. Erts, I. Iatsunskyi, A. Ramanavicius, Photoluminescence immunosensor based on bovine leukemia virus proteins immobilized on the ZnO nanorods, Sens. Actuators B, 2019, 285, 601-606.

[26] J. du Preez, D. Stephan, M. Mawassi, J. T. Burger, The grapevine-infecting vitiviruses, with particular reference to grapevine virus A, Arch. Virol. 156 (2011) 1495–1503.

[27] A. Ramanaviciene, V. Snitka, R. Mieliauskiene, R. Kazlauskas, A. Ramanavicius, AFM study of complement system assembly initiated by antigen-antibody complex, Cent.Eur.J.Chem. 4, 194 (2006) 194–206.

Graphical Abstract